Check for updates

Received: 10 March 2021 | Revised: 11 May 2021 | Accepted: 20 May 2021

DOI: 10.1002/ar.24697

SPECIAL ISSUE ARTICLE

The Anatomical Record

WILEY

Biomechanical performance of the cranio-mandibular complex of the small notosuchian *Araripesuchus gomesii* (Notosuchia, Uruguaysuchidae)

Mauro N. Nieto[1] | **Federico J. Degrange**[1] | **Kaleb C. Sellers**[2] | **Diego Pol**[3] | **Casey M. Holliday**[2]

[1]Centro de Investigaciones en Ciencias de la Tierra (CICTERRA), UNC, CONICET, Córdoba, Argentina

[2]Department of Pathology and Anatomical Sciences, University of Missouri, Columbia, Missouri

[3]Museo Paleontológico Egidio Feruglio-CONICET, Trelew, Chubut, Argentina

Correspondence
Mauro N. Nieto, Centro de Investigaciones en Ciencias de la Tierra (CICTERRA), UNC, CONICET, Avenida Vélez Sársfield 1611, X5016GCA, Córdoba, Argentina.
Email: mnicolasnieto@hotmail.com

Funding information
Agencia Nacional de Promoción Cientifica y Tecnológica, Fondo para la Investigación Científica y Tecnológica, Grant/Award Number: PICT 1319; Consejo Nacional de Investigaciones Científicas y Técnicas, Grant/Award Number: PUE 2016; National Science Foundation, Grant/Award Number: EAR 1631684

Abstract

Notosuchia is a clade of crocodyliforms that was highly successful and diverse in the Cretaceous of Gondwana. *Araripesuchus gomesii* is a small notosuchian from the Early Cretaceous of Brazil that belongs to Uruguaysuchidae, one of the subgroups of notosuchians that first radiated, during the Aptian–Albian. Here we present a finite element analysis of *A. gomesii* based on a model reconstructed from CT scans and performed using published bone properties for crocodiles. The adductor musculature and their respective attachment areas were reconstructed based on Extant Phylogenetic Bracket. Different functional scenarios were tested applying an estimated 158 N bite force: unilateral bite, bilateral bite, pullback, head-shake, and head-twist. The results obtained were compared with those of *Alligator mississippiensis*, one of its closest living relatives. In the different simulations, the skull and lower jaws of *Araripesuchus* suffers more stress in the head-shake movement, followed by the unilateral and pullback bites with stress focalized in the premaxillary region. In contrast, the head-twist is the one with smaller stress values. *Araripesuchus* possess an oreinirostral skull that may provide greater overall resistance in the different scenarios on average, unlike *Alligator* that has a platyrostral skull with less resistance to dorsoventral mechanical loads. Previous hypotheses that considered *A. gomesii* as omnivorous coupled with our results, its small size, and likely limited bite force, suggest this taxon probably fed on small prey and other trophic items that could catch and handle entirely with its mouth, such as insects and small vertebrates.

KEYWORDS

Araripesuchus, biomechanics, finite element analysis, Notosuchia, paleobiology

1 | INTRODUCTION

Notosuchia is a clade of terrestrial crocodyliforms mostly registered in Gondwana from the Aptian to the Miocene. This clade was remarkably successful during the Cretaceous and had high morphological disparity (Pol et al., 2014) and taxonomic diversity (Pol & Leardi, 2015), including taxa of small (e.g., *Araripesuchus* Price, 1959) to large body masses (e.g., *Baurusuchus* Price, 1945). Notosuchians have been interpreted as entirely terrestrial

 © 2021 American Association for Anatomy.

animals, having terminal nostrils, lateral orbits, and limbs with sagittal posture (Gasparini, 1971; Pol, 2005; Ősi, 2014), and possessed a great dental disparity. The dental diversity within the group suggests diverse trophic habits (Melstrom & Irmis, 2019; Ősi, 2014; Sellers, Schmiegelow, & Holliday, 2019; Stubbs, Pierce, Rayfield, & Anderson, 2013), from carnivorous (Gasparini, Chiappe, & Fernández, 1991; Godoy, Montefeltro, Norell, & Langer, 2014; Riff & Kellner, 2011) to omnivorous (Bonaparte, 1991; Nobre, Carvalho, de Vasconcellos, & Souto, 2008), and even herbivorous (Buckley, Brochu, Krause, & Pol, 2000; Kley et al., 2010; Wu & Sues, 1996). Cubo et al. (2020), based on paleohistological analyses, have recently proposed that notosuchians would have been ectothermic animals, similar to what is observed in extant Crocodylia and Lepidosauria.

Araripesuchus gomesii was one of the first notosuchians described from South America (Price, 1959). Subsequently, five other species were referred to this genus based on specimens from different regions of Gondwana, including Argentina (*A. patagonicus* Ortega, Gasparini, Buscalioni, & Calvo, 2000, and *A. buitreraensis* Pol & Apesteguía, 2005), Niger (*Araripesuchus wegeneri* Buffetaut, 1981, and *Araripesuchus rattoides* Sereno & Larsson, 2009), and Madagascar (*Araripesuchus tsangatsangana* Turner, 2006). Recent phylogenetic analyses have retrieved *Araripesuchus* as closely related to *Anatosuchus* from Niger (Sereno & Larsson, 2009) and *Uruguaysuchus* from Uruguay (Soto, Pol, & Perea, 2011) conforming the clade Uruguaysuchidae, which is registered from the Albian to Campanian–Maastrichtian (Pol & Leardi, 2015 and references therein). Uruguaysuchids have been depicted in most analyses as a basal clade of Notosuchia, and represents one of the earliest diversification events of Notosuchia in the "middle" Cretaceous of Gondwana (Pol et al., 2014). This clade is characterized by small body size (Godoy, Benson, Bronzati, & Butler, 2019), the presence of a short oreinirostral (domed snout) skull, long anterior palpebral, subcircular supratemporal fenestra, and a broadly concave mandibular symphysis. Particularly, *A. gomesii* has some degree of heterodonty, with small incisiviforms, a large maxillary caniniform, and buccolingually flattened posterior teeth with small marginal denticles. Few studies have explored the dietary habits of the different species of *Araripesuchus*. However, based on tooth morphology, presence of abrasion-type wear facets and inferences on mandibular movement it has been considered that these taxa were likely omnivorous (Ősi, 2014; Sereno & Larsson, 2009), with the possibility for one of the species, *A. wegeneri*, of being entirely herbivorous.

Morpho-functional analysis on notosuchians is scarce. Ősi (2014) carried out a work on biomechanical aspects in heterodont crocodyliforms, in which only some notosuchians were included. However, his work was based on simple muscle reconstructions. Montefeltro, Lautenschlager, Godoy, Ferreira, and Butler (2020) recently performed a finite element analysis (FEA) in *Baurusuchus*, but this taxon is a derived representative of the clade that is highly modified due to its specialization to carnivory. *A. gomesii* is an underived taxon in the group that shows a more plesiomorphic craniomandibular anatomy, such as a still present antorbital fenestra and a secondary palate only incipiently developed unlike extant Crocodylia. A biomechanical approach for this taxon could allow a better understanding of the different food specializations within the group.

Here we present a biomechanical analysis of the cranio-mandibular complex of *A. gomesii*, the first performed for an uruguaysuchid notosuchian. Bite force calculations and different feeding scenarios were simulated in order to evaluate its performance during the feeding. Using FEA, we characterize the skull biomechanically and quantify functional similarities and differences between *Araripesuchus* and living crocodylians.

2 | MATERIALS AND METHODS

2.1 | Specimens

The specimen *A. gomesii* AMNH 24450 from the American Museum of Natural History, New York, was CT-scanned and restored virtually. This specimen consists of two slabs that contain different bones and fragments of the skull and mandible that were taphonomically bent out of shape, so a restoration was needed. Both slabs were scanned at the AMNH CT scanning facility (pixel size: 0.1046 mm, 170 kV, 1,000 μA). For comparison, we modeled a specimen of *Alligator mississippiensis*. We chose *A. mississippiensis* because this is a model species for herpetological and functional studies (e.g., Metzger, Daniel, & Ross, 2005; Porro et al., 2011; Porro, Metzger, Iriarte-Díaz, & Ross, 2013; Reed et al., 2011) and because it is a living representative of the crocodyliform lineage. CT scans of *Alligator* were obtained freely from WitmerLab webpage (https://people.ohio.edu/witmerl/lab.htm).

2.2 | Model construction

From the information obtained from the scans of the skull and jaw of *A. gomesii*, a 3D reconstruction was made through segmentation using the Materialise Mimics 18.0 software (Figure 1a). Due to deformation, when needed, bones (or part of bones) that were broken or dislocated were segmented individually, mirrored and

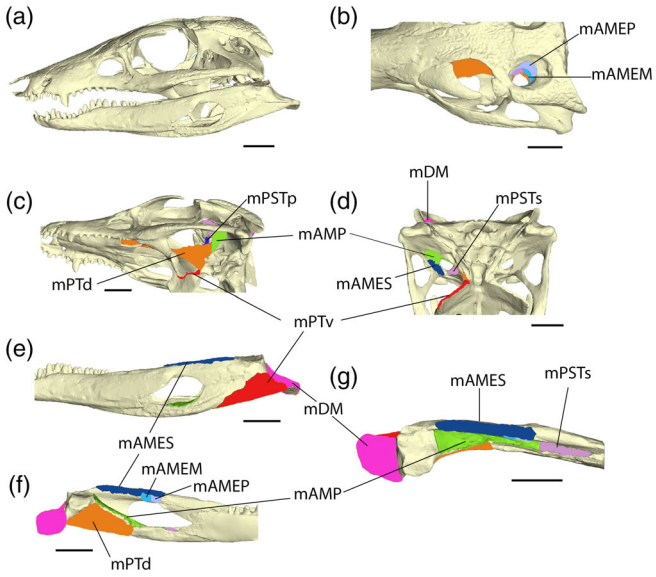

FIGURE 1 (a) Digitally restored skull and lower jaws in left lateral view of *Araripesuchus gomesii* AMNH 24450. (b–g) Muscle attachment areas marked on the 3D model skull of *A. gomesii*. (b) Dorsal view of the left posterior of the skull; (c) ventrolateral left view of the skull; (d) ventral view of the braincase; (e) left lateral view of the posterior portion of the mandibular ramus; (f) medial view of the posterior portion of the left mandibular ramus; (g) occlusal view of the posterior portion of the left mandibular ramus. mAMEM, m. adductor mandibulae externus medialis; mAMEP, m. adductor mandibulae externus profundus; mAMES, m. adductor mandibulae externus superficialis; mAMP, m. adductor mandibulae posterior; mDM, m. depressor mandibulae; mPSTp, m. pseudotemporalis profundus; mPSTs, m. pseudotemporalis superficialis; mPTd, m. pterygoideus dorsalis; mPTv, m. pterygoideus ventralis. Scale = 10 mm

merged with the rest of the skull. Stl files were brought into the software Geomagic (3D Systems) where they were corrected, eliminating small anatomical and geometrical errors in order to facilitate the construction of solid finite element meshes. Surface and volume meshes were generated in the 3-Matic Research module of Materialise. Meshes of the skull and jaw obtained (consisting of 519,080 bricks and 132,154 nodes for the skull, and 481,527 bricks and 105,769 nodes for the mandible) were imported to Strand7 Finite Element software (v. 2.3). Although 500,000 tetrahedra may be considered a bit low in convergence analyses for crania, the multiple analyses performed here justifies ~100,000 nodes/500,000 elements because solution time increases drastically at greater resolution. This resolution captures type and relative regional magnitudes of stress and strain, important for our comparisons between *Araripesuchus* and *Alligator*. Moreover, Gilbert, Snively, and Cotton (2016) found no gross differences comparing meshes of ~112,000 nodes/560,000 tetrahedra and 440,000 nodes/2 million elements, in a tarsometatarsus model that included slender internal structures. Models were assembled using 3D low order four-noded tetrahedral "brick" elements (tet4). In the original surface mesh, maximum and minimum triangle edge lengths were kept at a 1:3 ratio (0.1 geometric error) to minimize differences between triangle dimensions, which can lead to major discrepancies in brick element size in the final solid mesh introducing artifacts. Brick elements were assigned a single set of material properties published for *A. mississippiensis* (Young's modulus of Elasticity [E] = 8.8 GPa; Poisson's ratio = 0.4; Density = 1.0×10^{-6} kg/mm^3; Zapata et al., 2010). All the properties were assigned in the Strand7 software and treated as isotropic and homogeneous (i.e., assuming constant material properties throughout). Taking into account that the specimen of *Araripesuchus* needed restoration, and in the absence of data on material properties of notosuchians cranial tissues, we initially assigned isotropic materials because it has proven to (a) being available as determined in the literature, (b) having little effect on stress (but not directional strains) compared with anisotropic properties, and (c) accurately recovering general stress patterns (Strait et al., 2005).

2.3 | Muscle reconstruction and modeling

The adductor muscle and their respective attachment areas were reconstructed (Figure 1) based on Extant Phylogenetic Bracket (Witmer, 1995). Muscle attachments in *A. gomesii* were found to be largely similar in location as in *Alligator* (Sellers, Middleton, Davis, & Holliday, 2017), other crocodyliforms (Holliday & Witmer, 2009) and notosuchian crocodyliforms (e.g., Montefeltro et al., 2020; Ősi, 2014) with a few discrepancies. We did not find evidence for a significant attachment of m. pterygoideus ventralis on the medial surface of the articular as reconstructed in *Baurusuchus* (Montefeltro et al., 2020) and found m. pterygoideus dorsalis to attach along the medial surface of the caudal surangular and articular rather than in the Meckelian fossa and dorsal surface of the articular (sensu Montefeltro et al., 2020) or the rostral portion of the medial surface of the surangular in *Mariliasuchus* (sensu Ősi, 2014). Muscles were modeled as pre-tensioned trusses connecting each origin-insertion area, with an elastic modulus set to 0.1 MPa reflecting the modulus of relaxed muscle (McHenry, Wroe, Clausen, Moreno, & Cunningham, 2007; Moreno et al., 2008). The muscle forces were estimated using the attachment reconstructed area for each muscle, based on previous works on extant and extinct crocodyliforms

(Holliday, Tsai, Skiljan, George, & Pathan, 2013; Holliday & Witmer, 2007, 2009; Iordansky, 1964). Surface areas were used to calculate the volume of a frustum and published muscle architecture data of *A. mississippiensis* from Porro et al. (2011) were used to estimate the physiological cross sectional area (PCSA) of each muscle. Together, these attachment areas and PCSAs were used to calculate muscle forces after Sellers et al. (2017). Following previous muscle reconstructions in extant crocodilians (Holliday & Witmer, 2007; Sellers et al., 2017), the cartilago transiliens was not modeled here. In contrast, the musculus pseudotemporalis superficialis (mPSTs) and the musculus intramandibularis (mIM) were considered as a single muscle (mPSTs) that extends from the site of origin of mPSTs to the surface of insertion of mIM. The cartilago transiliens is a fibrocartilaginous element that acts as a union point between mPSTs and mIM, with collagenous fibers that extends from one muscle to the other with a cartilaginous disk connecting them (Tsai & Holliday, 2011). Therefore, the digital modeling is anatomically and mechanically similar to the in vivo muscle complex.

The analyzed skulls of *Araripesuchus* and *Alligator* differ in shape and size. In order to compare the performance and focus on how shape affects mechanical performance for a given loading condition, scaled values for the muscular contraction pressure need to be assumed. Based on this premise, *Alligator*'s models and forces were scaled to the total volume of the *A. gomesii* model following Dumont, Grosse, and Slater (2009) and Fortuny et al. (2015, 2016).

2.4 | Simulations

Models were restrained to prevent free body motion. For each loading, we have applied more realistic constraints by positioning them within frameworks of rigid links at the occipital condyle as well as at the tip of each teeth where bite force was applied. This was done in order to distribute forces more broadly. For the skull, three nodes were constrained on the occipital condyle following Montefeltro et al. (2020). To model the articular-quadrate joint, a hinged beam was used to link the upper and lower jaws. von Mises stresses were then used to compare performance among models. von Mises stresses are good predictors of failure under ductile fracture, or fractures that begin initially by plastic deformation, which is typically how bone fails. It is a function of principal stresses that measures how stress distorts a material (Rowe & Snively, 2021; Tsafnat & Wroe, 2011). Stress distribution and magnitude depend on the shape, size and force loading things that are well constrained in this work.

Different functional scenarios were tested to evaluate the cranio-mandibular biomechanical performance, simulating different situations of trophic item handling (Figure 2): unilateral bite, bilateral bite, pull-back, head-shake, and head-twist. Based on the availability of in vivo bite force measurements in extant crocodylians, we decided to use an estimated bite force (instead of force reactions) in the present study to simulate bite scenarios and compare the biomechanical performance with that of *Alligator*. For each one of these scenarios, the bite force was calculated based on Meers (2002), with a resulting bite force of 158.23 N. In the unilateral bite scenario, the loads were applied to a node, on different following teeth, perpendicular to the occlusion planes: premaxillary tooth 2 (PM2)-dentary tooth 1 (D1), maxillary tooth 3 (M3)-D7, and M8-D13 (Figure 2c–e). For the pull-back, the 158.23 N load was applied to one node at crown mid-height over the distal carina of the caniniform teeth (D5, PM3, and M3; Figure 2f,g). The bilateral bite was tested with two vectors of 79.115 N that were applied in each D6 and M3 (Figure 2h). The head-shake scenario was tested with four vectors of 79.115 N, two on each node on the labial surface of left M3/D5 and the other two on each node on the lingual surface of right M3/D5 (Figure 2i). Choosing a different dentary tooth in this simulation is due to the position of the rigid links on D6. For the head twist, the loadings were applied as two opposite vectors of 158.23 N in both jaw and skull models (Figure 2j): one loading vector was applied to one node at the tip of the maxillary (M3) and dentary (D8) caniniform tooth, and another loading vector on the opposite side on the dorsal surface of the maxilla, and ventral surface of the dentary, respectively. The protocol of the different scenarios performed followed that of Montefeltro et al. (2020).

These simulation scenarios were also tested in the skull and jaw of *A. mississippiensis* for comparisons. The unilateral bite was tested in PM3-D3, M4-D9, and M8-D13. The bilateral bite in both M4 and D9. The head shake and head twist scenario were also applied in M4 and D9. The pullback scenario was tested in PM3, M4, D3, and D9 (Figure 2b).

In order to compare the stress concentrated in the different regions of the skull both qualitatively and quantitatively, stresses from 10 landmark points were collected from the different bite scenarios following three transects, being the top of the skull following the midsagittal plane, the lateral part of the skull on the maxilla and jugal bar, and the lateral part of the mandible (Tables 1 and 2). The collection of von Mises stresses from these landmarks allows comparisons of values at homologous points in different models (Evans, Parr, Clausen, Jones, & Wroe, 2012; Parr et al., 2012).

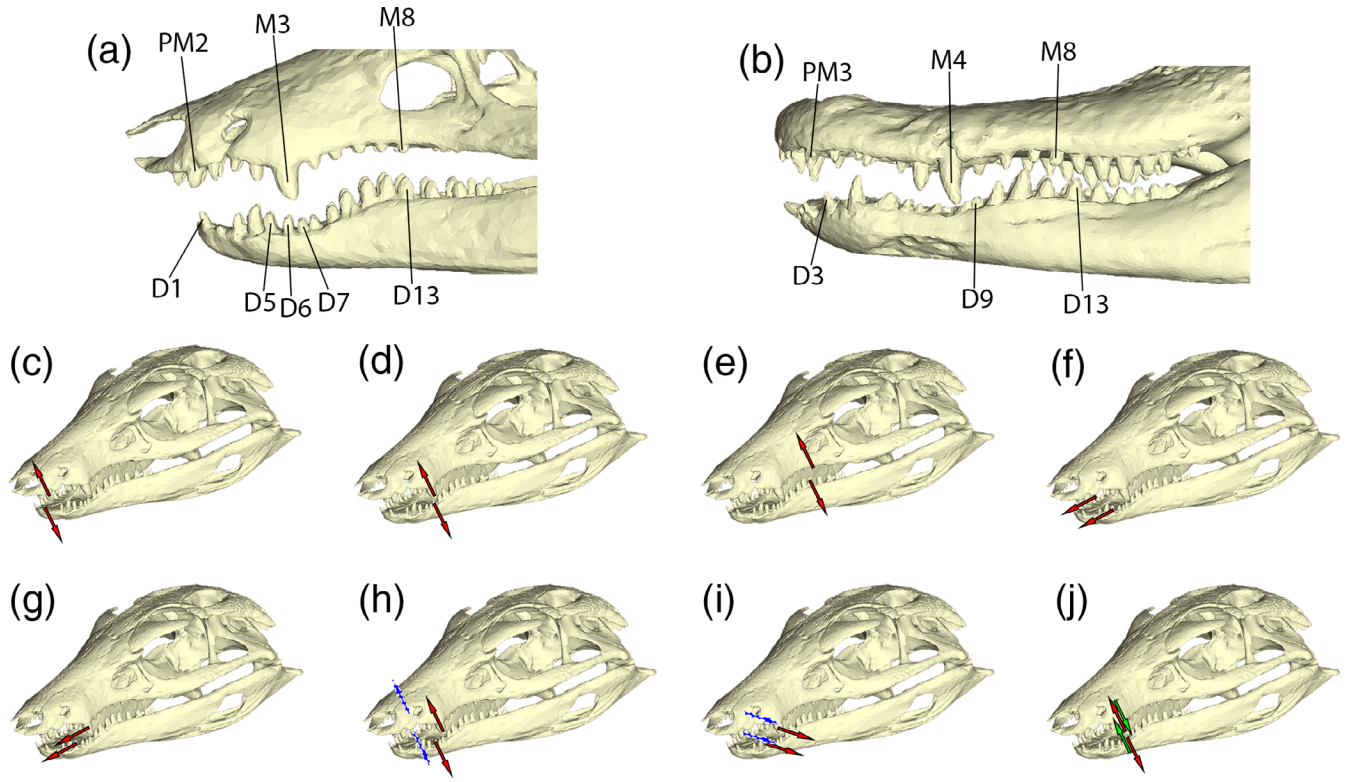

FIGURE 2 Different simulation of biting behavior in *Araripesuchus gomesii*. The arrows indicate the location on the models of the loading vectors for each scenario. (a) Lateral view of the snout of *A. gomesii* indicating the teeth involved in each simulation; (b) Lateral view of the snout of *Alligator mississippiensis* indicating the teeth involved in each simulation; (c) unilateral bite in premaxillary tooth 2 and dentary tooth 1; (d) unilateral bite in maxillary tooth 3 and dentary tooth 7; (e) unilateral bite in maxillary tooth 8 and dentary 13; (f) pullback bite in premaxillary tooth 3 and dentary tooth 5; (g) pullback bite in maxillary tooth 3 and dentary tooth 5; (h) bilateral bite in maxillary tooth 3 and dentary tooth 6; (i), head shake in maxillary tooth 3 and dentary tooth 5; (j) head twist in maxillary tooth 3 and dentary tooth 8. Red arrows indicate the force applied in the left side of the skull. Blue arrows with dotted line indicate the force applied in the right side of the skull. Green arrow indicate the force applied in the surface of the dentary and the surface of the maxilla

3 | RESULTS

The simulations for the different scenarios in *Araripesuchus* show a generalized pattern in which stress is mostly concentrated on the rostral area (maxilla, nasal, part of the jugal and lacrimal) and on the posterior part of the skull (Figure 3a–h). This is similar to the results obtained for *Alligator*, although in this taxon there is a higher concentration of stress in these regions (Figure 3i–p). The braincase of *Araripesuchus* is also a region with high concentration of stress, especially in the head shake scenario (Figure 3g) in which the overall stress values are much higher than in other scenarios. A similar result was obtained in the head-shake scenario for *Alligator* (Figure 3o). Nevertheless, in all scenarios the area of the cranial roof in *A. gomesii* had a lower stress concentration than in *A. mississippiensis* (Figures 3 and 4b, f) (Tables 1 and 2). In almost all scenarios, the tip of the snout and jaw of *Araripesuchus* showed lower stress levels than the rest of the skull and mandible (Figure 4b) (Table 1). Throughout the mandible, the stress in *A. gomesii* is quite homogeneous (Figure 4d) (Table 1). However, in the unilateral bite scenario using PM2 and D1 (Figure 3a) and in the two pullback scenarios (Figure 3d,e), the highest level of stress is concentrated on the dentary, especially on its dorsolateral region. The latter has also been retrieved for *Alligator*, although in the unilateral bite scenarios with PM2 and D1, and M3 and D7, the high stress is also present on the angular and surangular (Figures 3i,j and 4d). In both taxa our results indicate that the posterior end of the retroarticular process is under low stress.

In the scenarios involving unilateral bites (Figures 3a–e) there generally is an asymmetry in the stress distribution, with higher stresses shifted towards the working side. The scenarios in which the skull of *Araripesuchus* is most affected correspond to those of the unilateral bite with PM2 and D1, pull back with M3 and D5, and headshake (Figure 3a,e,g), the latter being the one with the highest stress concentrated in the posterior area of the skull, including the braincase, the quadrate, quadratojugal, and jugal

TABLE 1 Measured points for the different bites scenarios in *Araripesuchus gomesii*

	Measured point	Biting scenario							
		Uni1	Uni2	Uni3	Pullpmx	Pullmx	Bilat	Head shake	Head twist
Midsagittal plane of the skull	1	0.51	0.022	0.014	0.14	0.13	1.56	0.09	0.003
	2	12.99	0.96	2.38	7.19	5.21	7.57	7.10	1.03
	3	24.99	4.77	7.07	11.64	10.40	16.41	8.15	1.03
	4	29.74	12.96	11.46	11.12	15.39	9.75	6.60	1.90
	5	18.11	11.21	9.59	9.20	9.84	2.10	5.15	0.86
	6	16.22	9.65	5.13	10.38	7.36	1.14	7.90	1.58
	7	14.08	13.58	10.75	8.60	9.90	1.12	15.90	2.30
	8	8.28	2.24	6.97	3.17	3.19	1.00	22.90	0.90
	9	5.50	3.15	1.61	2.97	3.67	0.98	4.65	1.25
	10	1.14	1.26	1.55	2.96	2.53	1.24	6.64	0.80
Lateral of the skull	1	0.01	0.00	0.00	0.00	0.00	0.05	0.05	0.00
	2	26.00	12.75	11.88	21.20	5.38	18.69	9.70	0.84
	3	5.14	20.17	4.48	10.80	31.20	10.42	26.70	2.78
	4	58.00	20.17	35.47	15.10	33.30	12.83	24.70	6.43
	5	8.21	9.14	11.36	5.95	12.00	11.43	31.70	5.39
	6	2.41	3.55	1.35	2.47	2.47	3.96	20.30	1.26
	7	3.10	1.45	4.24	2.15	3.58	6.57	27.10	1.61
	8	1.92	8.54	1.55	1.09	2.55	5.90	20.00	2.42
	9	6.60	15.57	14.54	12.70	21.10	25.12	21.20	8.39
	10	4.53	6.46	7.11	8.33	7.11	6.41	8.60	3.93
Lateral of the Lower jaws	1	151.14	0.36	0.36	1.90	7.63	8.61	5.79	0.08
	2	2.28	12.80	5.27	26.40	28.00	27.00	12.40	5.54
	3	37.10	15.40	10.10	36.20	39.20	11.60	8.73	4.62
	4	40.02	13.80	6.21	35.40	38.40	12.70	6.39	6.73
	5	34.18	20.90	5.07	30.70	31.50	10.70	19.10	2.35
	6	11.16	11.30	17.90	8.79	8.69	9.39	16.20	4.45
	7	4.22	12.70	6.27	10.20	11.20	10.90	25.10	6.32
	8	7.27	7.76	2.59	22.70	22.70	23.00	26.10	12.00
	9	11.44	14.20	2.15	16.10	10.50	3.55	24.60	13.00
	10	0.65	0.42	0.34	0.55	11.40	0.23	0.22	0.19

Note: All values are expressed in MegaPascal (MPa) of von Mises stress. Abbreviations: Uni1, unilateral bite in premaxillary tooth 2 and dentary tooth 1; Uni2, unilateral bite in maxillary tooth 3 and dentary tooth 7; Uni3, unilateral bite in maxillary tooth 8 and dentary tooth 13; Pullpmx, pullback bite in premaxillary tooth 3 and dentary tooth 5; Pullmx, pullback bite in maxillary tooth 3 and dentary tooth 5; Bilat, bilateral bite in maxillary tooth 3, and dentary tooth 6.

(Figure 4b,c) (Table 1). In *Alligator*, the scenario with the greatest stress is registered in the unilateral bite with PM3 and D3 (Figures 3i and 4f,g) (Table 2). Conversely, the scenario that registers the lower stress values in *Araripesuchus* is the head twist (Figures 3h and 4c,d), in which the calculated stress levels in general do not exceed 5 MPa (Figure 4b–d) (Table 1). In the same way, our results for *A. mississippiensis* also indicate this scenario is the one with the smallest stress values (Figures 3p, 4f,g) (Table 2).

4 | DISCUSSION

4.1 | Skull performance

Based on previous analyses on the mandibular movement and tooth wear pattern, the species of *Araripesuchus* have been considered as omnivores, with a possible case of herbivory in *A. wegeneri* (Ősi, 2014; Sereno & Larsson, 2009; Turner, 2006). These hypotheses were

TABLE 2 Measured points for the different bites scenarios in *Alligator mississippiensis*

	Measured point	Biting scenario							
		Uni1	Uni2	Uni3	Bilat	Pullpmx	Pullmx	Head shake	Head twist
Midsagittal plane of the skull	1	22.20	1.72	7.33	4.76	16.65	2.69	17.65	0.80
	2	10.47	3.41	4.76	8.87	6.73	10.66	13.34	2.13
	3	43.82	13.76	18.65	17.27	11.88	16.75	18.84	3.43
	4	47.73	22.21	20.45	16.72	17.77	19.13	8.95	3.61
	5	53.09	20.21	21.16	14.87	17.82	20.45	9.18	4.60
	6	47.23	22.24	16.05	8.10	16.68	13.71	6.48	3.39
	7	37.52	17.93	17.01	5.68	9.28	21.47	15.07	2.40
	8	15.07	27.86	11.09	1.75	16.13	16.15	20.62	0.93
	9	38.41	11.11	7.42	0.79	17.18	8.11	11.45	2.17
	10	17.65	4.59	9.83	5.98	21.44	26.45	12.51	1.88
Lateral of the skull	1	8.02	1.17	5.21	6.70	14.65	1.79	24.54	0.37
	2	27.38	8.60	56.87	14.61	27.43	4.04	8.91	1.99
	3	23.91	52.85	9.11	16.41	18.28	69.38	17.35	18.83
	4	46.21	55.89	27.01	16.02	22.72	36.04	21.50	5.44
	5	83.84	21.04	17.50	4.85	24.31	19.47	16.74	1.11
	6	30.40	7.67	9.80	3.36	9.67	9.55	30.46	0.91
	7	38.95	9.88	18.37	5.22	12.23	15.30	57.49	13.06
	8	32.58	8.34	4.56	8.62	4.51	16.41	6.92	30.31
	9	44.94	19.28	13.00	7.02	20.83	23.06	27.53	27.42
	10	20.94	16.64	11.12	3.30	8.21	9.70	9.58	18.60
Lateral of the lower jaws	1	108.52	84.30	4.09	10.31	39.05	7.62	64.74	2.28
	2	61.24	44.09	22.84	32.41	58.71	18.73	87.12	10.96
	3	78.61	44.54	40.37	18.81	75.38	40.35	78.54	23.45
	4	143.14	71.71	3.26	20.70	30.50	46.22	38.84	6.65
	5	108.66	76.18	46.90	27.34	39.65	52.79	28.68	5.04
	6	79.34	62.35	8.81	10.65	27.09	38.02	20.32	2.85
	7	59.89	54.06	14.23	9.32	3.16	4.28	31.46	2.18
	8	68.74	71.21	20.25	7.92	8.18	12.90	69.51	1.06
	9	33.01	71.60	13.03	3.27	28.19	32.58	18.22	6.29
	10	0.63	0.62	0.63	0.43	0.66	0.44	0.50	0.39

Note: All values are expressed in MegaPascal (MPa) of von Mises stress. Abbreviations: Uni1, unilateral bite in premaxillary tooth 3 and dentary tooth 3; Uni2, unilateral bite in maxillary tooth 4 and dentary tooth 9; Uni3, unilateral bite in maxillary tooth 8 and dentary tooth 13; Pullpmx, pullback bite in premaxillary tooth 3 and dentary tooth 3; Pullmx, pullback bite in maxillary tooth 4 and dentary tooth 9; Bilat, bilateral bite in maxillary tooth 4 and dentary tooth 9.

based on anatomical observations on the skull, mandible, and teeth of these taxa. However, since form and functions are sometimes decoupled, functional analyses can provide complementary information on feeding habits. The biomechanical analysis carried out here shows that the skull of *Araripesuchus* would be better suited to perform dorsoventral and anteroposterior movements than movements with a strong lateral component.

Alligator and *Araripesuchus* are phylogenetically related but they represent two distinct lineages within Crocodyliformes (Neosuchia and Notosuchia, respectively) that have markedly different skull morphology. Whereas *A. mississippiensis* has a characteristically platyrostral skull, *A. gomesii* has an oreinirostral (domed snout) skull. The platyrostral skull is a derived character that appeared in evolution of Neosuchia (Rayfield &

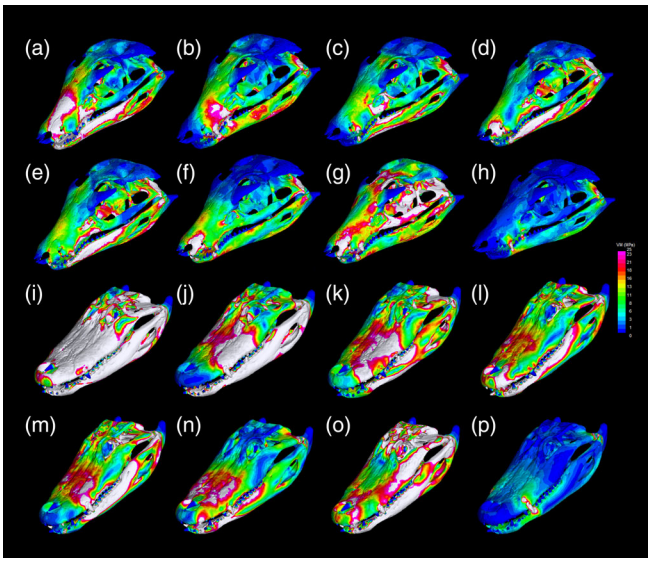

FIGURE 3 Stress (von Mises) distribution in *Araripesuchus gomesii* (a–h) and *Alligator mississippiensis* (i–p). (a) Unilateral bite in premaxillary tooth 2 and dentary tooth 1; (b) unilateral bite in maxillary tooth 3 and dentary tooth 7; (c) unilateral bite in maxillary tooth 8 and dentary tooth 13; (d) pullback bite in premaxillary tooth 3 and dentary tooth 5; (e) pullback bite in maxillary tooth 3 and dentary tooth 5; (f) bilateral bite in maxillary tooth 3 and dentary tooth 6; (g) head shake in maxillary tooth 3 and dentary tooth 5; (h) head twist in maxillary tooth 3 and dentary tooth 8; (i), unilateral bite in premaxillary tooth 3 and dentary tooth 3; (j) unilateral bite in maxillary tooth 4 and dentary tooth 9; (k) unilateral bite in maxillary tooth 8 and dentary 13; (l) pullback bite in premaxillary tooth 3 and dentary tooth 3; (m) pullback bite in maxillary tooth 4 and dentary tooth 9; (n) bilateral bite in maxillary tooth 4 and dentary tooth 9; (o) head shake in maxillary tooth 4 and dentary tooth 9; (p) head twist in maxillary tooth 4 and dentary tooth 9. Warm colors indicate high stress and cool colors indicate region of low stress. Areas shown in white exceed the scale maximum (25 MPa). Note that the scenarios in which the skull of *Araripesuchus* show higher stress concentration correspond to those of the unilateral bite with PM2 and D1, pull back with M3 and D5, and head-shake

Milner, 2008) and was probably linked to the acquisition of aquatic habits (McHenry, Clausen, Daniel, Meers, & Pendharkar, 2006; Wilberg et al., 2019). Busbey (1995) suggested that the adaptation of crocodiles to a platyrostral form is related to the increment in the resistance of torsional loads in the skull, and the decrease in hydrodynamic resistance in lateral movements during feeding. With this premise, previous studies analyzed the importance of the presence/absence of the antorbital fenestra and the secondary palate in the different types of skulls (platyrostral and oreinirostral) in Crocodylomorpha (e.g., McHenry et al., 2006; Rayfield & Milner, 2008). In the evolution of this group, there is a drastic change from the condition of early crocodylomorphs (e.g., *Sphenosuchus acutus*) with a large antorbital fenestra and absence of a complete secondary palate to that of crown crocodylians (e.g., *A. mississippiensis*) that lack antorbital fenestra and have complete secondary palate. *Araripesuchus* provides an interesting intermediate stage in which the antorbital fenestra is still present but the secondary palate is incipiently developed (with the participation of the maxilla and palatines). Similarly to what was concluded in other studies (Busbey, 1995; McHenry et al., 2006; Rayfield & Milner, 2008), the oreinirostral snout of *Araripesuchus* seems to provide greater resistance during feeding than the platyrostral snout of *A. mississippiensis*, despite presenting an antorbital fenestra, which would represent a zone of "weakness" in the skull (Rayfield & Milner, 2008). However, this zone may be complemented by the development of the secondary palate in notosuchians, reducing the stress concentration (see McHenry et al., 2006; Rayfield & Milner, 2008).

The stress distribution shows that *Alligator* have, in general, higher von Mises stress in the mandible (Figures 3 and 4). Porro et al. (2011) demonstrates that the symphysis is an area of high torsional stress and its strong interdigitation could help to mitigate this. *Araripesuchus* possess a more robust symphyseal region that would surely help to stabilize the lower jaws at the time of the bite, generating less stress (see Figures 3 and 4). This is also observed in an advanced notosuchian like *Baurusuchus* (Montefeltro et al., 2020) that has an even longer symphysis.

Although it is not an emphasis of the present work, under pullback scenarios (Figure 3d,e), the modeled *A. gomesii* experiences high levels of stress in the quadrate region. Ortega et al. (2000) observed that in this region the articular is larger than the condyle of the quadrate, suggesting a potential anteroposterior movement, which is later observed in more advanced notosuchians such as *Notosuchus terrrestris* (Lecuona & Pol, 2008), generating a stress release in this area.

4.2 | FEA in other notosuchians

The morphological and ecological diversity of notosuchians was remarkably high but functional studies are still scarce. Montefeltro et al. (2020) conducted a FEA for *Baurusuchus*, a notosuchian that differs markedly in its skull anatomy from *Araripesuchus*. In addition to its larger overall body size, the skull of *Baurusuchus* has a much narrower and higher rostrum, absence of an antorbital fenestra, and dentition composed of only five large maxillary teeth with serrated carinae (resembling those of theropods). Montefeltro et al. (2020) showed that *Baurusuchus* had better biomechanical performance with less stress than *Alligator* and *Allosaurus* in the

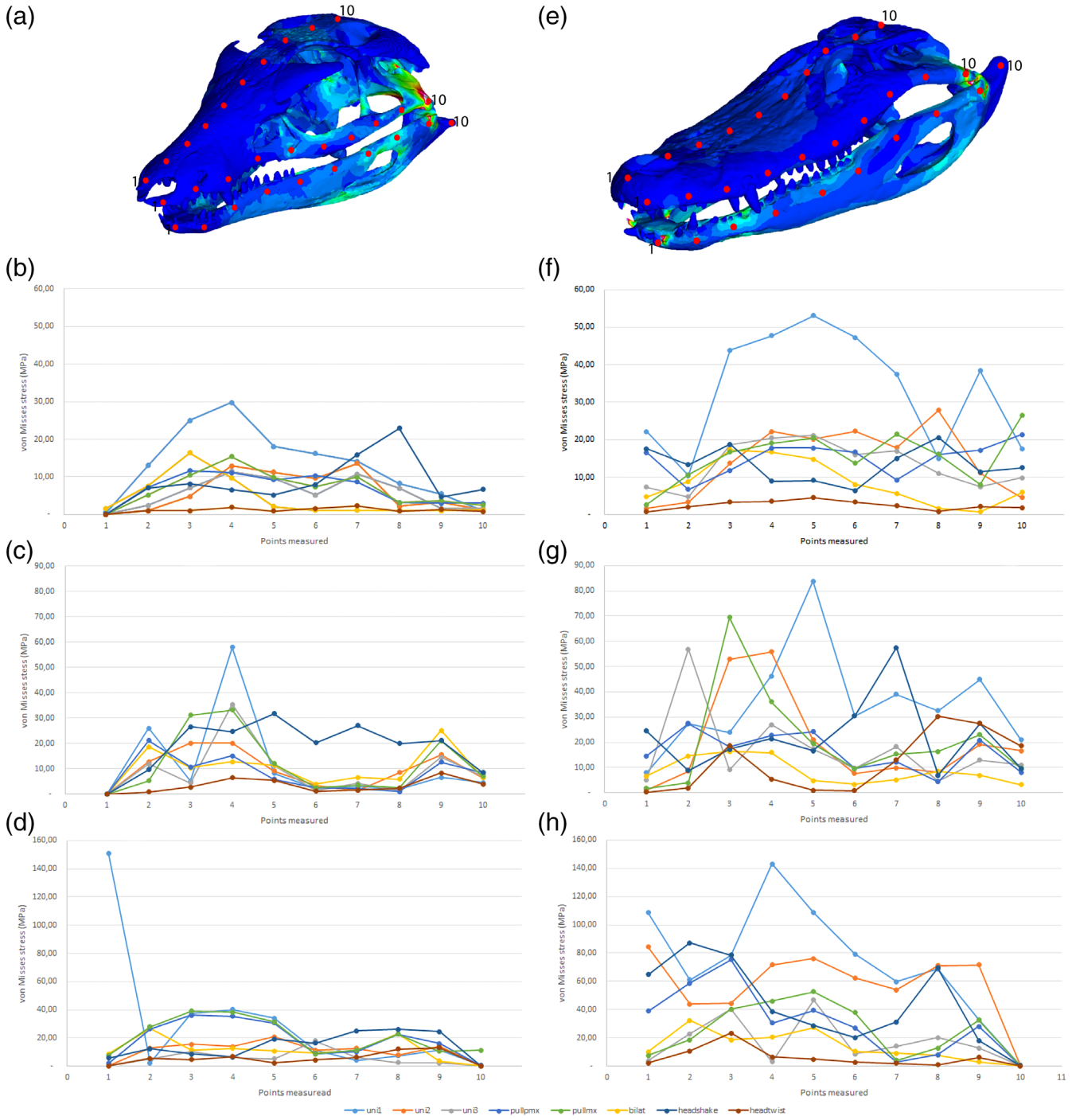

FIGURE 4 Stress measurements along a the skull of *Araripesuchus gomesii* (a–d) and *Alligator mississippiensis* (e–h) on the sagittal plane, lateral of the skull and the lateral of the lower jaws during the different biting simulations. *Araripesuchus* (a) and *Alligator* (e) skulls showing the location of the measurement points; (b and f) stress values measured for each simulation on the sagittal plane; (c and g) stress values measured for each simulation on the lateral of the skull; (d and h), stress values measured for each simulation on the lateral of the lower jaw. Abbreviations as in Tables 1 and 2. Note that in the different bite scenarios, in general, *Araripesuchus* present lower levels of stress, especially in the head twist and bilateral scenarios

premaxillary–maxillary region. This may be because *Baurusuchus* lacks an antorbital fenestra, a characteristic related to greater resistance to various efforts like torsion loads and bending scenarios (Rayfield & Milner, 2008). This greater resistance could be related to the trophic habit inferred for *Baurusuchus*, considered as a top predator (Godoy et al., 2014; Riff & Kellner, 2011), and it would represent a great advantage when catching prey

and the effort generated when handling larger prey (Montefeltro et al., 2020 and citations therein). Feeding imposes strong selective pressure on skull morphology, even leading to specialization, and *Baurusuchus* seems to respond to this mechanisms.

A more comprehensive study was preliminary reported by Srinivas, Rayfield, Tavares, Cunningham, and Vargas (2019), who carried out finite element analyses on various Notosuchia and compared results with those for extant Crocodylia. The results reported are consistent with those obtained in the present analysis. Although the calculated forces for the bite and bone properties are different, from those used here the observed results patterns are similar. Srinivas et al. (2019) noted that oreinirostral morphologies are better suited for resisting force during biting, which is coincident with our findings for *Araripesuchus*.

4.3 | Paleobiology

The specimen of *A. gomesii* (AMNH 24450) is a slightly smaller individual than the holotype, barely exceeding 50 cm in total length. Since there is a relationship between body mass and bite force (Christiansen & Wroe, 2007; Meers, 2002), it is not surprising that its inferred bite force is relatively small. In comparison with extant taxa of similar size and weight, such as the mammals South American gray fox (*Lycalopex griseus*) and the pampas fox (*Lycalopex gymnocerus*), or the lizard gold tegu (*Tupinambis teguixin*), the inferred bite force of *Araripesuchus* reaches similar ranges to these taxa (approximately 130–150 N; Anderson, McBrayer, & Herrel, 2008; Christiansen & Wroe, 2007). Based on our results on the stress distribution pattern, however, it is also possible that the skull of *Araripesuchus* would be able to withstand a greater bite force, especially when performing a head twist movement (Figure 3h).

Despite these studies, there is still much of the paleobiology and behavior of Notosuchia that remains unexplored. *A. gomesii* had a straight posture and has been described as a terrestrial animal (Hecht, 1991). It has functionally heterodont dentition but a precise tooth–tooth occlusion was absent or possibly only have relative occlusion during the orthal movements of the jaw (Ősi, 2014). The presence of wear facets are more related to abrasion from tooth-food contact than to precise tooth-tooth occlusion (Ősi, 2014; Sereno & Larsson, 2009). In extant Crocodylia, diet varies throughout its ontogeny (Gignac & O'Brien, 2016; Grigg & Kirshner, 2015; Tucker, Limpus, McCallum, & McDonald, 1996): hatchlings and juveniles are generalists, feeding on insects, mollusks, crustaceans and small fish and frogs, adding larger animals as they grow (larger fish, birds, and mammals). Ontogenetic dietary shifts are probably also true for other crocodyliforms such as *Araripesuchus* (Sereno & Larsson, 2009). Sereno and Larsson (2009) and Ősi (2014) postulated that *Araripesuchus* was an omnivore mainly based on the absence of dental specialization for either carnivory or herbivory. The results presented here seem are compatible with this hypothesis, in which the animal fed on small prey and other items that could be caught entirely with its mouth and easy to manipulate. Lower stresses in bilateral (Figure 3d) than for unilateral bite simulations (Figure 3a–c) suggest the likelihood of this behavior. As observed in extant lepidosaurs (e.g., *Varanus komodoensis*) and inferred in *Baurusuchus*, the use of the cervical musculature and appendicular motions can provide an increase in the force exerted on the trophic item, complementing the bite force (D'Amore & Blumenschine, 2009; D'Amore, Moreno, McHenry, & Wroe, 2011; McHenry et al., 2007; Montefeltro et al., 2020; Moreno et al., 2008). These features would help to dissipate and potentially tolerate larger stress along other body parts, such as those required for capturing and holding larger prey items. Most species of Crocodylia and Lepidosauria are mostly solitary hunters, but some species repeatedly engaged in behaviors classified as "cooperative" or "protocooperative" which allows different individuals to feed on the same prey (Dinets, 2015; Grigg & Kirshner, 2015). Although there is no evidence of cooperative behavior in notosuchians, these small crocodyliforms may have used similar behavior if larger prey were part of their diet. Nevertheless, more evidence and research in these aspects are necessary for determinate this kind of behavior.

ACKNOWLEDGMENTS

Editors Jeffrey Laitman, Casey Holliday, and Emma Schachner are thanked for the invitation to participate in the special issue "The Age of Crocodiles: Anatomy, Physiology and Evolution". Eric Snively and an anonymous reviewer are thanked for their helpful comments and suggestions. We are grateful with CONICET for constant support. This is a contribution to PICT 1319, and PUE 2016-CONICET-CICTERRA. Thanks to National Science Foundation EAR 1631684.

AUTHOR CONTRIBUTIONS

Mauro Nieto: Conceptualization; formal analysis; investigation; methodology; writing-original draft; writing-review & editing. **Kaleb Sellers:** Investigation; methodology; writing-review & editing. **Casey Holliday:** Funding acquisition; investigation; writing-review & editing. **Federico Degrange:** Conceptualization; formal

analysis; funding acquisition; investigation; methodology; writing-review & editing. **Diego Pol:** Funding acquisition; investigation; writing-review & editing.

ORCID

Mauro N. Nieto https://orcid.org/0000-0003-4245-4425
Federico J. Degrange https://orcid.org/0000-0002-9463-4893
Kaleb C. Sellers https://orcid.org/0000-0002-3588-9562
Diego Pol https://orcid.org/0000-0002-9690-7517
Casey M. Holliday https://orcid.org/0000-0001-8210-8434

REFERENCES

Anderson, R. A., McBrayer, L. D., & Herrel, A. (2008). Bite force in vertebrates: Opportunities and caveats for use of a nonpareil whole-animal performance measure. *Biological Journal of the Linnean Society*, *93*, 709–720.

Bonaparte, J. F. (1991). Los vertebrados fósiles de la formación Río Colorado, de la ciudad de Neuquén y sus cercanías, Cretácico superior, Argentina. *Revista del Museo Argentino de Ciencias Naturales "Bernardino Rivadavia". Paleontología*, *4*, 17–123.

Buckley, G. A., Brochu, C. A., Krause, D. W., & Pol, D. (2000). A pug-nosed crocodyliform from the late cretaceous of Madagascar. *Nature*, *405*, 941–944.

Buffetaut, E. (1981). Die biogeographische Geschichte der Krokodilier, mit Beschreibungeiner neuen Art, Araripesuchus wegneri. *Geologische Rundschau*, *70*, 611–624.

Busbey, A. B. (1995). The structural consequences of skull flattening in crocodilians. In J. J. Thomason (Ed.), *Functional morphology in vertebrate paleontology* (pp. 173–192). Cambridge: Cambridge University Press.

Christiansen, P., & Wroe, S. (2007). Bite forces and evolutionary adaptations to feeding ecology in carnivores. *Ecology*, *88*(2), 347–358.

Cubo, J., Sena, M. V. A., Aubier, P., Houee, G., Claisse, P., Faure-Brac, M. G., ... Oliveira, G. R. (2020). Were Notosuchia (Pseudosuchia: Crocodylomorpha) warm-blooded? A palaeohistological analysis suggest ectothermy. *Biological Journal of the Linnean Society*, *131*, 154–162.

D'Amore, D. C., & Blumenschine, R. J. (2009). Komodo monitor (*Varanus komodoensis*) feeding behavior and dental function reflected through tooth marks on bone surfaces, and the application to ziphodont paleobiology. *Paleobiology*, *35*, 525–552.

D'Amore, D. C., Moreno, K., McHenry, C. R., & Wroe, S. (2011). The effects of biting and pulling on the forces generated during feeding in the Komodo dragon (*Varanus komodoensis*). *PLoS One*, *6*(10), e26226.

Dinets, V. (2015). Apparent coordination and collaboration in cooperatively hunting crocodilians. *Ethology Ecology & Evolution*, *27* (2), 244–250.

Dumont, E. R., Grosse, I. R., & Slater, G. J. (2009). Requirements for comparing the performance of finite element models of biological structures. *Journal of Theoretical Biology*, *256*, 96–103.

Evans, S. P., Parr, W. C. H., Clausen, P. D., Jones, A., & Wroe, S. (2012). Finite element analysis of a micromechanical model of bone and a new 3D approach to validation. *Journal of Biomechanics*, *45*, 2702–2705.

Fortuny, J., Marcé-Nogué, J., Heiss, E., Sanchez, M., Gil, L., & Galobart, À. (2015). 3D bite modeling and feeding mechanics of the largest living amphibian, the chinese giant salamander *Andrias davidianus* (Amphibia: Urodela). *PLoS One*, *10*(4), e0121885.

Fortuny, J., Marcé-Nogué, J., Steyer, J. S., de Esteban-Trivigno, S., Mujal, E., & Gil, L. (2016). Comparative 3D analyses and palaeoecology of giant early amphibians (Temnospondyli: Stereospondyli). *Scientific Reports*, *6*(1), 30387.

Gasparini, Z. (1971). Los Notosuchia del Cretácico de América del Sur como un nuevo infraorden de los Mesosuchia (Crocodilia). *Ameghiniana*, *8*(2), 83–103.

Gasparini, Z., Chiappe, L., & Fernández, M. (1991). A new Senonian peirosaurid (Crocodylomorpha) from Argentina and a synopsis of the South American cretaceous crocodilians. *Journal of Vertebrate Paleontology*, *11*, 316–333.

Gignac, P., & O'Brien, H. (2016). Suchian feeding success at the interface of ontogeny and macroevolution. *Integrative and Comparative Biology*, *56*, 449–458.

Gilbert, M. M., Snively, E., & Cotton, J. (2016). The tarsometatarsus of the ostrich *Struthio camelus*: Anatomy, bone densities, and structural mechanics. *PLoS One*, *11*, e0149708.

Godoy, P. L., Benson, R. B. J., Bronzati, M., & Butler, R. (2019). The multipeak adaptive landscape of crocodylomorph body size evolution. *BMC Evolutionary Biology*, *19*, 167.

Godoy, P. L., Montefeltro, F. C., Norell, M. A., & Langer, M. C. (2014). An additional baurusuchid from the cretaceous of Brazil with evidence of interspecific predation among crocodyliformes. *PLoS One*, *9*, e97138.

Grigg, G., & Kirshner, D. (2015). *Biology and evolution of Crocodylians*. Melbourne: Csiro Publishing.

Hecht, M. (1991). Araripesuchus Price, 1959. In J. G. Maisey (Ed.), *Santana fossils: An illustrated atlas* (pp. 342–347). Neptune, NJ: T.F.H. Publications.

Holliday, C. M., Tsai, H., Skiljan, R., George, I., & Pathan, S. (2013). A 3D interactive model and atlas of the jaw musculature of *Alligator mississippiensis*. *PLoS One*, *8*, e62806.

Holliday, C. M., & Witmer, L. M. (2007). Archosaur adductor chamber evolution: Integration of musculoskeletal and topological criteria in jaw muscle homology. *Journal of Morphology*, *268*, 457–484.

Holliday, C. M., & Witmer, L. W. (2009). The epipterygoid of crocodyliforms and its significance for the evolution of the orbitotemporal region of eusuchians. *Journal of Vertebrate Paleontology*, *29*, 715–733.

Iordansky, N. (1964). The jaw muscles of the crocodiles and some relating structures of the crocodilian skull. *Anatomischer Anzeiger*, *115*, 256–280.

Kley, N. J., Sertich, J. J. W., Turner, A. H., Krause, D. W., O'Connor, P. M., & Georgi, J. A. (2010). Craniofacial morphology of *Simosuchus clarki* (Crocodyliformes: Notosuchia) from the late cretaceous of Madagascar. *Journal of Vertebrate Paleontology*, *30*, 1–89.

Lecuona, A., & Pol, D. (2008). Tooth morphology of *Notosuchus terrestris* (Notosuchia: Mesoeucrocodylia): New evidence and implications. *Comptes Rendus Palevol*, *7*, 407–417.

McHenry, C. R., Clausen, P. D., Daniel, W. J. T., Meers, M. B., & Pendharkar, A. (2006). Biomechanics of the rostrum in crocodilians: A comparative analysis using finite element analysis. *The Anatomical Record*, *288A*, 827–849.

McHenry, C. R., Wroe, S., Clausen, P. D., Moreno, K., & Cunningham, E. (2007). Supermodeled sabercat, predatory behaviour in *Smilodon fatalis* revealed by highresolution 3-D computer simulation. *PNAS*, *104*, 16010–16015.

Meers, M. B. (2002). Maximum bite force and prey size of *Tyrannosaurus rex* and their relationship to the inference of feeding behaviour. *Historical Biology*, *16*, 1–12.

Melstrom, M. K., & Irmis, R. B. (2019). Repeated evolution of herbivorous Crocodyliforms during the age of dinosaurs. *Current Biology*, *29*(14), 2389–2395.

Metzger, K. A., Daniel, W. J. T., & Ross, C. F. (2005). Comparison of beam theory and finite-element analysis with in vivo bone strain data from the Alligator cranium. *The Anatomical Record*, *283A*, 331–348.

Montefeltro, F. C., Lautenschlager, S., Godoy, P. L., Ferreira, G. S., & Butler, R. J. (2020). A unique predator in a unique ecosystem: Modelling the apex predator within a late cretaceous crocodyliform-dominated fauna from Brazil. *Journal of Anatomy*, *237*, 323–333.

Moreno, K., Wroe, S., Clausen, P. D., McHenry, C. R., D'Amore, D. C., Rayfield, E. J., & Cunningham, E. (2008). Cranial performance in the Komodo dragon (*Varanus komodoensis*) as revealed by high-resolution 3-D finite element analysis. *Journal of Anatomy*, *212*, 736–746.

Nobre, P. H., Carvalho, I. S., de Vasconcellos, F. M., & Souto, P. R. (2008). Feeding behavior of the Gondwanic Crocodylomorpha *Mariliasuchus amarali* from the Upper Cretaceous Bauru Basin, Brazil. *Gondwana Research*, *13*, 139–145.

Ortega, F., Gasparini, Z., Buscalioni, A. D., & Calvo, J. O. (2000). A new species of *Araripesuchus* (Crocodylomorpha, Mesoeucrocodylia) from the lower Cretaceous of Patagonia (Argentina). *Journal of Vertebrate Paleontology*, *20*, 57–76.

Ősi, A. (2014). The evolution of jaw mechanism and dental function in heterodont crocodyliforms. *Historical Biology*, *26*, 279–414.

Parr, W., Wroe, S., Chamoli, U., Richards, H. S., McCurry, M., Clausen, P. D., & McHenry, C. (2012). Toward integration of geometric morphometrics and computational biomechanics: New methods for 3D virtual reconstruction and quantitative analysis of Finite Element Models. *Journal of Theoretical Biology*, *301*, 1–14.

Pol, D. (2005). Postcranial remains of *Notosuchus terrestris* Woodward (Archosauria: Crocodyliformes) from the Upper Cretaceous of Patagonia, Argentina. *Ameghiniana*, *42*, 21–38.

Pol, D., & Apesteguía, S. (2005). New *Araripesuchus* remains from the Early Late Cretaceous (Cenomanian-Turonian) of Patagonia. *Amer Mus Nov*, *3490*, 1–38.

Pol, D., & Leardi, J. (2015). Diversity patterns of Notosuchia (Crocodyliformes, Mesoeucrocodylia) during the cretaceous of Gondwana. In M. Fernández & Y. Herrera (Eds.), *Reptiles Extintos – Volumen en Homenaje a Zulma Gasparini* (Vol. 15, pp. 172–186). Buenos Aires: Publicación Electrónica de la Asociación Paleontológica Argentina.

Pol, D., Nascimento, P., Carvalho, M., Riccomini, A. B., Pires-Domingues, R. A., & Zaher, H. (2014). A new notosuchian from the Late Cretaceous of Brazil and the phylogeny of advanced notosuchians. *PLoS One*, *9*, e93105.

Porro, L. B., Holliday, C. M., Anapol, F., Ontiveros, L. C., Ontiveros, L. T., & Ross, C. F. (2011). Free body analysis, beam mechanics, and finite element modeling of the mandible of *Alligator mississippiensis*. *Journal of Morphology*, *272*, 910–937.

Porro, L. B., Metzger, K. A., Iriarte-Díaz, J., & Ross, C. F. (2013). In vivo bone strain and finite element modelling of the mandible of *Alligator mississippiensis*. *Journal of Anatomy*, *223*, 195–227.

Price, L. I. (1945). A new reptile from the cretaceous of Brazil. *Notas Preliminares e Estudos. Servicio Geologia Mineralogia do Brasil*, *25*, 1–8.

Price, L. I. (1959). Sobre um crocodilideo notossuquio do Cretáceo Brasileiro. *Boletim Divisão de Geologia e Mineralogia Rio de Janeiro*, *118*, 1–55.

Rayfield, E., & Milner, A. (2008). Establishing a framework for archosaur cranial mechanics. *Paleobiology*, *34*, 494–515.

Reed, D. A., Porro, L. B., Iriarte-Díaz, J., Lemberg, J. B., Holliday, C. M., Anapol, F., & Ross, C. F. (2011). The impact of bone and suture material properties on mandibular function in *Alligator mississippiensis*: Testing theoretical phenotypes with finite element analysis. *Journal of Anatomy*, *218*, 59–74.

Riff, D., & Kellner, A. (2011). Baurusuchid crocodyliforms as theropod mimics: Clues from the skull and appendicular morphology of *Stratiotosuchus maxhechti* (upper cretaceous of Brazil). *Zoological Journal of the Linnean Society*, *163*(suppl 1), S37–S56.

Rowe, A. J., & Snively, E. (2021). Biomechanics of juvenile tyrannosaurid mandibles and their implications for bite force: Evolutionary biology. *The Anatomical Record*, 1–20. https://doi.org/10.1002/ar.24602

Sellers, K. C., Middleton, K., Davis, J., & Holliday, C. M. (2017). Ontogeny of bite force in a validated biomechanical model of the American alligator. *The Journal of Experimental Biology*, *220*, 2036–2046.

Sellers, K. C., Schmiegelow, A. B., & Holliday, C. M. (2019). The significance of enamel thickness in the teeth of *Alligator mississippiensis* and its diversity among crocodyliforms. *Journal of Zoology*, *9*(3), 172–181.

Sereno, P. C., & Larsson, H. C. E. (2009). Cretaceous Crocodyliforms from the Sahara. *ZooKeys*, *28*, 1–143.

Soto, M., Pol, D., & Perea, D. (2011). A new specimen of *Uruguaysuchus aznarezi* (Crocodyliformes: Notosuchia) from the middle cretaceous of Uruguay and its phylogenetic relationships. *Zoological Journal of the Linnean Society*, *163*, S173–S198.

Srinivas, A., Rayfield, E. J., Tavares, S. A. S., Cunningham, J. A., & Vargas, K. (2019). Constraints and adaptations in crocodilian skull form and function. *PaleoBios*, *36*, 334.

Strait, D. S., Wang, Q., Dechow, P. C., Ross, C. F., Richmond, B. G., Spencer, M. A., & Patel, B. A. (2005). Modelling elastic properties in finite-element analysis: How much precision is needed to produce an accurate model? *The Anatomical Record*, *283A*, 275–287.

Stubbs, T. L., Pierce, S. E., Rayfield, E. J., & Anderson, P. S. L. (2013). Morphological and biomechanical disparity of crocodile-line archosaurs following the end-Triassic extinction. *Proceedings of the Royal Society B*, *280*, 20131940.

Tsafnat, N., & Wroe, S. (2011). An experimentally validated micromechanical model of a rat vertebra under compressive loading. *Journal of Anatomy*, *218*, 40–46.

Tsai, H. P., & Holliday, C. M. (2011). Ontogeny of the alligator cartilago transiliens and its significance for sauropsid jaw muscle evolution. *PLoS One*, *6*, e24935.

Tucker, A. D., Limpus, C. J., McCallum, H. I., & McDonald, K. R. (1996). Ontogenetic dietary partitioning by *Crocodylus johnstoni* during the dry season. *Copeia*, *1996*, 978–988.

Turner, A. H. (2006). Osteology and phylogeny of a new species of *Araripesuchus* (Crocodyliformes: Mesoeucrocodylia) from the late cretaceous of Madagascar. *Historical Biology*, *18*, 255–369.

Wilberg, E. W., Turner, A. H., & Brochu, C. A. (2019). Evolutionary structure and timing of major habitat shifts in Crocodylomorpha. *Scientific Reports*, *9*(1), 514. https://doi.org/10.1038/s41598-018-36795-1.

Witmer, L. M. (1995). The extant phylogenetic bracket and the importance of reconstructing soft tissues in fossils. In J. J. Thomason (Ed.), *Functional morphology in vertebrate paleontology* (pp. 19–33). New York: Cambridge University Press.

Wu, X.-C., & Sues, H.-D. (1996). Anatomy and phylogenetic relationships of *Chimaeresuchus paradoxus*, an unusual crocodyliform reptile from the Lower Cretaceous of Hubei, China. *Journal of Vertebrate Paleontology*, *16*, 688–702.

Zapata, U., Metzger, K., Wang, Q., Elsey, R. M., Ross, C. F., & Dechow, P. C. (2010). Material properties of mandibular cortical bone in the American alligator, *Alligator mississippiensis*. *Bone*, *46*, 860–867.

How to cite this article: Nieto, M. N., Degrange, F. J., Sellers, K. C., Pol, D., & Holliday, C. M. (2021). Biomechanical performance of the cranio-mandibular complex of the small notosuchian *Araripesuchus gomesii* (Notosuchia, Uruguaysuchidae). *The Anatomical Record*, 1–13. https://doi.org/10.1002/ar.24697